Nat. Hazards Earth Syst. Sci., 12, 2225–2240, 2012
www.nat-hazards-earth-syst-sci.net/12/2225/2012/
doi:10.5194/nhess-12-2225-2012

Natural Hazards and Earth System Sciences

Analysis of intense rainfall events on Madeira Island during the 2009/2010 winter

F. T. Couto[1], **R. Salgado**[1,2], **and M. J. Costa**[1,2]

[1]Évora Geophysics Centre – CGE, Évora, Portugal
[2]Physics Department, University of Évora, Évora, Portugal

Correspondence to: F. T. Couto (couto.ft@gmail.com)

Received: 17 January 2012 – Revised: 20 March 2012 – Accepted: 16 May 2012 – Published: 19 July 2012

Abstract. This paper constitutes a step towards the understanding of some characteristics associated with high rainfall amounts and flooding on Madeira Island. The high precipitation events that occurred during the winter of 2009/2010 have been considered with three main goals: to analyze the main atmospheric characteristics associated with the events; to expand the understanding of the interaction between the island and the atmospheric circulations, mainly the effects of the island on the generation or intensification of orographic precipitation; and to evaluate the performance of high resolution numerical modeling in simulating and forecasting heavy precipitation events over the island. The MESO-NH model with a horizontal resolution of 1 km is used, as well as rain gauge data, synoptic charts and measurements of precipitable water obtained from the Atmospheric InfraRed Sounder (AIRS). The results confirm the influence of the orographic effects on precipitation over Madeira as well as the tropical–extratropical interaction, since atmospheric rivers were detected in six out of the seven cases analyzed, acting as a low level moisture supplier, which together with the orographic lifting induced the high rainfall amounts. Only in one of the cases the presence of a low pressure system was identified over the archipelago.

1 Introduction

Orographic precipitation is one of the strongest evidences of interaction between the surface and the atmosphere. The mechanisms responsible for orographic precipitation development or enhancement are reported in several studies (e.g. Smith, 1979; Houze, 1993; Roe, 2005). The different mechanisms of orographic precipitation can be associated with stable and convective precipitation or amplification of an existing precipitation (also known as the seeder-feeder mechanism; Bergeron, 1950, 1968), depending on some factors, for example, size/shape of the mountain, moisture content, stability of the airmass, and large-scale disturbances. Mountains usually modify, and often amplify, rather than create precipitation (Smith, 2006). Aiming at a better representation of precipitation over complex terrain, Smith and Barstad (2004) developed the linear model of orographic precipitation, considering airflow dynamics, cloud time scales and advection, and downslope evaporation, which may be easily applied in complex terrains (e.g. Caroletti and Barstad, 2010).

Sometimes, orographic precipitation can be observed as heavy rainfall, causing several damages, landslides or floods. Within this context, orographic precipitation has been investigated in many studies around the globe. Lin et al. (2001) summarized some common synoptic and mesoscale environments responsible for heavy rainfall events in the United States, the European Alps, and East Asia. Nevertheless, most of the studies have been developed for mountainous regions located in mid-latitudes, for example, under the Mesoscale Alpine Programme (MAP; Bougeault et al., 2001; Rotunno and Houze, 2007) and the Convective and Orographically-induced Precipitation Study (COPS; Barthlott et al., 2011; Richard et al., 2011; Wulfmeyer et al., 2011). Costa et al. (2010) identified the important role of orography in the distribution of precipitation over the Iberian Peninsula, with enhancement in the regions with mountain ranges and diminution over certain valleys.

Many studies have confirmed the important role played by the meridional water flux, also known as Atmospheric Rivers (ARs), which favors the intensification of orographic precipitation. Atmospheric rivers are long ($>\sim$2000 km), narrow

(<∼1000 km wide) bands of enhanced water vapor flux (e.g. Ralph et al., 2004; Neiman et al., 2008a, b), which can produce heavy rainfall when striking the coastal mountains, through orographic lifting. Zhu and Newell (1998) found that the majority of the mid-latitudes moisture flux occurs in the filamentary features, the rivers, and that the fraction of the globe they cover is 10 % or less. In the literature, these structures were often known as warm conveyor belts (Carlson, 1991). From observational studies, Ralph et al. (2004) characterized narrow regions of strong horizontal water vapor flux associated with polar cold fronts that occurred over the eastern North Pacific Ocean during the winter of 1997/1998.

Neiman et al. (2008b) documented the high impact of ARs on an extreme precipitation event and flooding in the Pacific Northwest that occurred on November 2006. On the other hand, according to Ralph et al. (2006), while the presence of an atmospheric river was a necessary condition observed in 7 floods on the "Russian River" occurring during a period of 8 yr, it was not a sufficient condition to trigger the phenomena. Recently, Dettinger et al. (2011), investigating meteorological aspects of the connection between floods and water resources in California, observed that atmospheric rivers are a primary meteorological factor in flood generation of many California rivers, as well as a primary source of precipitation and water resources in the State, contributing with 20–50 % to the State's precipitation and streamflow. Stohl et al. (2008) analyzed an extreme precipitation event on the Norwegian southwest coast, which produced flooding and landslides, and found that it was triggered by the transport of (sub)tropical moisture through an atmospheric river rooted in the tropical western North Atlantic. The steep topography of the Norwegian coast caused strong orographic enhancement of the precipitation associated with the river. The authors showed that, unlike what has been reported in the literature, in this case some of the moisture was transported across more than 40° of latitude.

Heavy precipitation may cause huge economic losses as well as social problems (Chu et al., 2009). Therefore, several studies have been dedicated to orographic precipitation, especially over islands. For some tropical mountainous islands where maritime moist and winds with a predominant direction are constant, the orographic effects on the distribution and intensification of rainfall are well understood. On Hawaii, different studies have been carried out focusing on orographic precipitation (e.g. Kolivras and Comrie, 2007; Chu et al., 2010). Taiwan is another place where the orographic effects on rainfall distribution have been widely studied (e.g. Yeh and Chen, 1998; Kerns et al., 2010), as well as Dominica island, located in the Caribbean sea, where recently tropical orographic precipitation has been explored (e.g. Kirshbaum and Smith, 2009; Smith et al., 2009a, b). However, there are relatively few studies of orographic precipitation over Madeira Island. Tomé and Miranda (2007) studied a set of years with extreme weather conditions on Madeira using two mesoscale models (MM5 and WRF) and two simple downscaling models, but other aspects related to orographic precipitation over the island deserve more attention. Many studies developed for Madeira have focused on other meteorological aspects, such as fog precipitation and interception in the main forest types on Madeira (e.g. Prada et al., 2009), or on isolated case studies of high precipitation events (e.g. Luna et al., 2011).

The Madeira Archipelago is a group of Portuguese islands located in the North Atlantic Ocean and formed by two main inhabited islands, Madeira and Porto Santo. To the southeast the archipelago continues along the Desertas and Selvagens, both composed of three islands. Madeira is the largest island of the archipelago with an area of approximately 740 km^2, a length of 58 km and 23 km width. Centered at 32°75′ N and 17°00′ W, the mountainous island is completely formed by volcanic materials, consisting of an enormous east–west oriented mass that is cut by deep valleys (Prada and Silva, 2001). The island has a mountain ridge that extends mainly along the central part of the island with the highest peaks in the eastern part, Pico Ruivo (1862 m) and Pico do Areeiro (1818 m), while the Paúl da Serra region (above 1400 m) is located in the western part. This situation, location and steep topography, together with the natural vegetation, provide Madeira with a great variety of micro-climates, mostly Mediterranean climate, with mild summer and winter, except for the elevated regions where the lowest temperatures are observed (Santos and Miranda, 2006; Borges et al., 2008). The precipitation regime over the island is not only affected by local circulation, but also by synoptic systems typical of mid-latitudes, such as fronts and extratropical cyclones, and the Açores Anticyclone in the summer season.

This paper is a step towards the understanding of some aspects or atmospheric characteristics associated with high rainfall amounts and flooding on Madeira Island. For this purpose, the events that occurred during the winter of 2009/2010 have been considered with three main goals: (1) to analyze the main atmospheric characteristics associated with the events; (2) to expand the understanding of the interaction between the island and the atmospheric circulations, mainly the effects of the island on the generation or intensification of orographic precipitation; and (3) to evaluate the performance of high resolution numerical modeling to simulate and forecast heavy precipitation events over Madeira.

The structure of the paper is the following: in Sect. 2 the data used as well as the methodology are described. The rain gauge data, synoptic and satellite observations are examined and discussed in Sect. 3, together with the numerical simulations outputs. The conclusions are summarized in Sect. 4.

Table 1. Identification of the meteorological stations used in the work, presenting the number, name, location and altitude.

Number	Station	Short name	Latitude (° N)	Longitude (° W)	Altitude (m)
522	Funchal/Observatório	Funchal	32.6475	−16.8924	58
960	Santana/S. Jorge	Santana	32.8344	−16.9062	185
973	Areeiro	Areeiro	32.7166	−16.9166	1510
978	Caniçal/São Lourenço	Caniçal	32.7469	−16.7055	136
980	Lombo da Terça	Lombo Terça	32.8313	−17.2022	935
986	Ponta do Sol/Lugar de Baixo	Ponta Sol	32.6666	−17.0833	48
990	Calheta/Ponta do Pargo	Calheta	32.8138	−17.2632	312

2 Data and methods

2.1 Methodology

The method developed consists of three steps. The first step consists of the rainfall analysis from rain gauge data. The period of analysis of these data corresponds to the winter months of 2009/2010, i.e. December 2009, January and February 2010. Daily accumulated precipitation was computed from hourly data. The analysis of these data led to the choice of several case studies, selected based on the rainfall amounts. The case study identification was based mainly on the data from the Areeiro station, situated near the top of the island. The second part of the methodology comprises the large-scale analysis, carried out using synoptic surface charts and precipitable water maps obtained from AIRS satellite observations. These precipitable water maps for February were compared with the NCEP/DOE AMIP-II Reanalysis (Reanalysis-2), monthly average from 1979 to 2009 (http://www.esrl.noaa.gov). Finally, the last step consists of the numerical simulations of the four most intense cases that occurred during the study period. At this stage, besides the high resolution simulation of precipitation (mm), other variables were examined, such as the atmospheric stability from the Convective Available Potential Energy – CAPE ($J\,kg^{-1}$), the wind components ($m\,s^{-1}$), vertical velocity ($m\,s^{-1}$), cloud fraction, and the mixing ratio for rain, cloud water, ice, snow, and graupel ($g\,kg^{-1}$). This step includes a point to point comparison between the observed precipitation and the corresponding simulations, aiming to evaluate the model ability to reproduce heavy precipitation events on the island.

2.2 Synoptic analysis, rain gauge and satellite observations

The large-scale characteristics were identified through the analysis of synoptic meteorological charts for the North Atlantic Ocean and Europe provided by the Portuguese Meteorological Institute (Instituto de Meteorologia – IM). The data series of precipitation used in this study were collected at the Madeira meteorological stations belonging to the Portuguese Meteorological Institute. Daily amounts were extracted from hourly data for a total of 7 stations distributed over the island (Table 1 and Fig. 1).

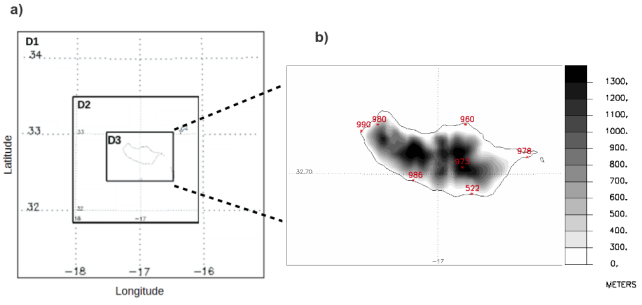

Fig. 1. (a) Horizontal domains used in the simulations with grid spacing of 9 km (D1), 3 km (D2) and 1 km (D3). **(b)** The shaded areas represent the 1km orography (m) obtained from the GTOPO30 database. Point (station): 522 (Funchal), 960 (Santana), 973 (Areeiro), 978 (Caniçal), 980 (Lombo da Terça), 986 (Ponta do Sol), 990 (Calheta).

The total precipitable water is used in this paper as support in large-scale analyses. The total precipitable water is obtained from the Atmospheric InfraRed Sounder (AIRS). The AIRS is one of six instruments on board the Aqua satellite, part of the NASA Earth Observing System. It has 2378 spectral channels with wavelengths ranging from 3.7 to 15.4 µm and 4 visible channels with wavelengths ranging from 0.4 to 0.94 µm (Parkinson, 2003). The AIRS has a spatial resolution of 13.5 km at nadir and a spectral resolution more than 100 times greater than previous IR sounders, providing more accurate information on the vertical profiles of atmospheric temperature and moisture (Aumann et al., 2003).

2.3 Model setup

The mesoscale non-hydrostatic model (MESO-NH; Lafore et al., 1998), which was used in this work, was jointly developed by the Centre National de Recherches Météorologiques (CNRM) and the Laboratoire d'Aerologie (Meteo-France). The MESO-NH is able to simulate the atmospheric motions, ranging from the large meso-alpha scale down to the micro-scale, using as prognostic variables the three components of the wind, the potential temperature, the

turbulent kinetic energy and up to seven classes of mixing ratios (r) for water substances, considering the vapor (r_v), liquid cloud water (r_c), liquid rain (r_r), cloud ice (r_i), snow (r_s), graupel (r_g) and hail (r_h). The MESO-NH model has been successfully used many times in quantitative precipitation forecasting (e.g. Nuissier et al., 2008). The model is implemented with three different anelastic models and a sigma-z vertical coordinate, where the lower level follows the topography and which is also known as the classical Gal-Chen and Sommerville (1975) coordinate. The grid used by the MESO-NH is the C-grid in the Arakawa convention, both on the horizontal and on the vertical. Currently, the grid nesting or two-way interactive grid nesting is implemented in the MESO-NH code with some modifications (Stein et al., 2000), allowing the simultaneous simulation of several scales of motion.

In addition to dynamic and thermodynamic equations, which govern the atmospheric motions, the MESO-NH is implemented with a rather complete parameterization package of several physical processes observed in the atmosphere. The surface energy exchanges are parameterized according to different schemes depending on the surface types (nature, urban, ocean, lake), included in the SURFEX package (e.g. Salgado and Le Moigne, 2010). It uses an enhanced soil-vegetation-atmosphere transfer scheme initially proposed by Noilhan and Planton (1989), known as ISBA (Interaction between Soil, Biosphere and Atmosphere Scheme). The orography is obtained from the gtopo30 database and the land cover is taken from the ecoclimap database (Masson et al., 2003). The ECMWF radiation package (Morcrette et al., 1986; Morcrette, 1991; Gregory et al., 2000) is used in order to parameterize the radiative transfer in the atmosphere. The package calculates the radiative fluxes taking into account absorption-emission of longwave radiation and reflection, scattering and absorption of solar radiation by the earth's atmosphere. The parameterization of turbulence was made by means of a 1.5 order closure one-dimensional scheme, using the Bougeault and Lacarrère (1989) mixing length. The convection was parameterized in the 9 km domain using the Bechtold et al. (2001) mass-flux scheme, which developed a model based on the traditional scheme of Kain and Fritsch (1993).

The MESO-NH provides several schemes for the parameterization of cloud microphysics, related to warm and cold clouds. In this work, the ICE3 scheme (Pinty and Jabouille, 1998) was activated, which provides the temporal evolution of mixing ratios of six water species and of the cloud fraction.

The numerical simulations were carried out with 45 vertical stretched levels and three horizontal nested domains (Fig. 1), in a two-way interactive mode. The larger domain (D1) was established with 40×40 grid points and a spacing of 9 km, the second domain (D2) with 60×60 grid points and a resolution of 3 km and the third domain (D3) with 90×60 grid points and a 1 km resolution. The area corresponding to the horizontal domains is presented in Fig. 1a

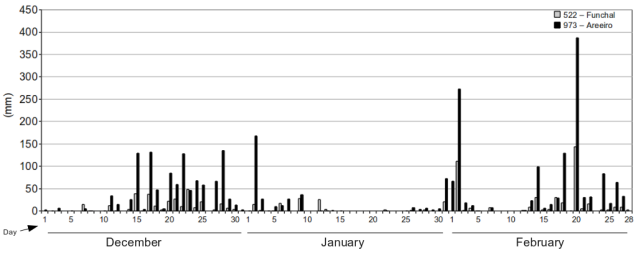

Fig. 2. Daily rainfall amounts obtained for Areeiro station (black) and Funchal station (gray) during the winter season (DJF) 2009/2010.

together with the 1 km resolution orography of the inner domain (Fig. 1b), centered over Madeira island. In diagnostic mode the initial and boundary conditions were updated every 6 h and obtained from the ECMWF analyses, while in prognostic mode these conditions were updated every 3 h from the ECMWF forecasts. The MESO-NH was run in diagnostic mode in all selected cases. For the 20 February 2010 catastrophe case, the model was also run in prognostic mode in order to test the performance of the MESO-NH forecast. The main features for each case are shown in Table 2.

3 Results and discussion

3.1 Rainfall analysis and large-scale environment

The analysis of the daily accumulated rainfall distribution for the winter 2009/2010 (DJF) in seven surface stations (not shown here) indicates that the maximum daily rainfall values are systematically recorded over Madeira's highlands. This characteristic may be confirmed when comparing the daily rainfall amounts between Areeiro and Funchal stations during the winter season (Fig. 2). Areeiro station is located at a height of 1510 m, whereas Funchal station, close to the sea, is at 58 m. The maximum values observed in Fig. 2 are clearly different between the two stations, the higher values being observed at Areeiro station, showing that the orography of the island plays an important role in rainfall distribution. Figure 2 also shows significant peaks with accumulated precipitation in Areeiro greater than 125 mm per day.

During December 2009, the maximum values in Areeiro station did not exceed 140 mm. There were 4 days with daily precipitation greater than 125 mm, different from the values observed at the other stations, where the maximum did not exceed 60 mm. In January 2010, a lower number of cases with significant precipitation was observed; however, one case with daily precipitation of 168.5 mm was identified in Areeiro. During the rest of the month there were no other records of significant rainfall amounts, the second maximum being 72.7 mm.

Table 2. Simulation dates and main features for each case.

CASE	Date	Period	Diagnostic mode Start (Time/Date)	Prognostic mode Start (Time/Date)
1	22 December 2009	54 h	00:00 UTC/21_Dec	–
2	28 December 2009	30 h	18:00 UTC/27_Dec	–
3	2 February 2010	54 h	00:00 UTC/01_Feb	–
4	20 February 2010	36 h	12:00 UTC/19_Feb	12:00 UTC/19_Feb

The distribution of rainfall for February was marked by two peaks representing rainfall amounts greater than 250 mm day^{-1} at Areeiro station, with a maximum of 273.1 mm on 2 February and another of 387.1 mm on 20 February 2010, the latter being the most intense case that occurred during the season. Within this context, a set of seven cases has been selected for analysis: 15 December 2009; 17 December 2009; 22 December 2009; 28 December 2009; 2 January 2010; 2 February 2010; and 20 February 2010.

The basic synoptic situation was evaluated from synoptic charts as shown in Fig. 3, where a frontal structure acting over Madeira's archipelago is evident. This figure represents the synoptic situation observed in the most intense case (20 February 2010) at 18:00 UTC, where the low-pressure area is centered at approximately 40° N and 17° W (north of Madeira), while the island is under the influence of the warm sector region and the passage of the cold front associated with this system. This kind of pattern was also verified in five other cases, meaning that in six (of seven) cases the synoptic conditions over the archipelago were strongly influenced by the passage of a frontal system, with the center of the cyclone located to the north of Madeira. The remaining case was characterized by the development of a low-pressure system over the southern part of the archipelago, being centered between Madeira and the Canary Islands. This case corresponds to the second most intense event, which occurred on 2 February 2010.

Another crucial factor also associated with the dynamics of the extratropical cyclones, related to large-scale circulation, was found in the precipitable water maps: the frequent existence of warm conveyor belts in the warm sector. This is an important structure in tropical–extratropical interaction, which transports heat and moisture from the tropics towards the mid-latitudes. Being coupled to frontal systems, the atmospheric rivers act as low level jets. Figure 4 shows that in six of the seven most intense precipitation events (selected cases) it is possible to verify the presence of a narrow band with high amounts of precipitable water, extending from the tropics, particularly from the Caribbean sea region, to the higher latitudes, namely the region of the Madeira Archipelago, in the pathway of these atmospheric rivers. Note that, unfortunately, on 22 December 2009 there was no satellite observation over the island; therefore the observation of 23 December 2009 is shown (Fig. 4c). Comparing the cases where the atmospheric rivers are present (Fig. 4a, b, c, d, e, and g), the satellite observations show that the amounts of precipitable water exceed in most of the cases 40 kg m^{-2} (i.e. Fig. 4d). In fact, sometimes the precipitable water reaches values greater than 50 kg m^{-2} (Fig. 4g). The fact that the synoptic pattern is similar for all but one of the high rainfall events indicates that the presence of atmospheric rivers has to be considered as an important aspect in the generation of high amounts of precipitation on the Island.

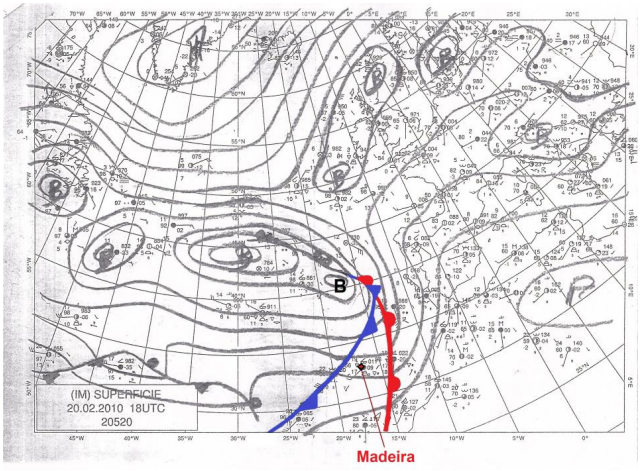

Fig. 3. Synoptic chart of surface pressure showing the large-scale pattern for the North Atlantic and Europe on 20 February 2010 at 18:00 UTC (provided by the Instituto de Meteorologia).

In the case of 2 February 2010, the atmospheric river, i.e. the meridional transport of heat and humidity, was not present (Fig. 4f). The synoptic situation was characterized by the presence of a low pressure system centered to the south of the island, which contained a large amount of precipitable water with values greater than 60 kg m^{-2} near the island. Note that the precipitable water amounts in the selected cases are about two or sometimes three times higher than the thirty year average value (1979–2009) obtained for the month of February from the NCEP reanalysis and shown in Fig. 5.

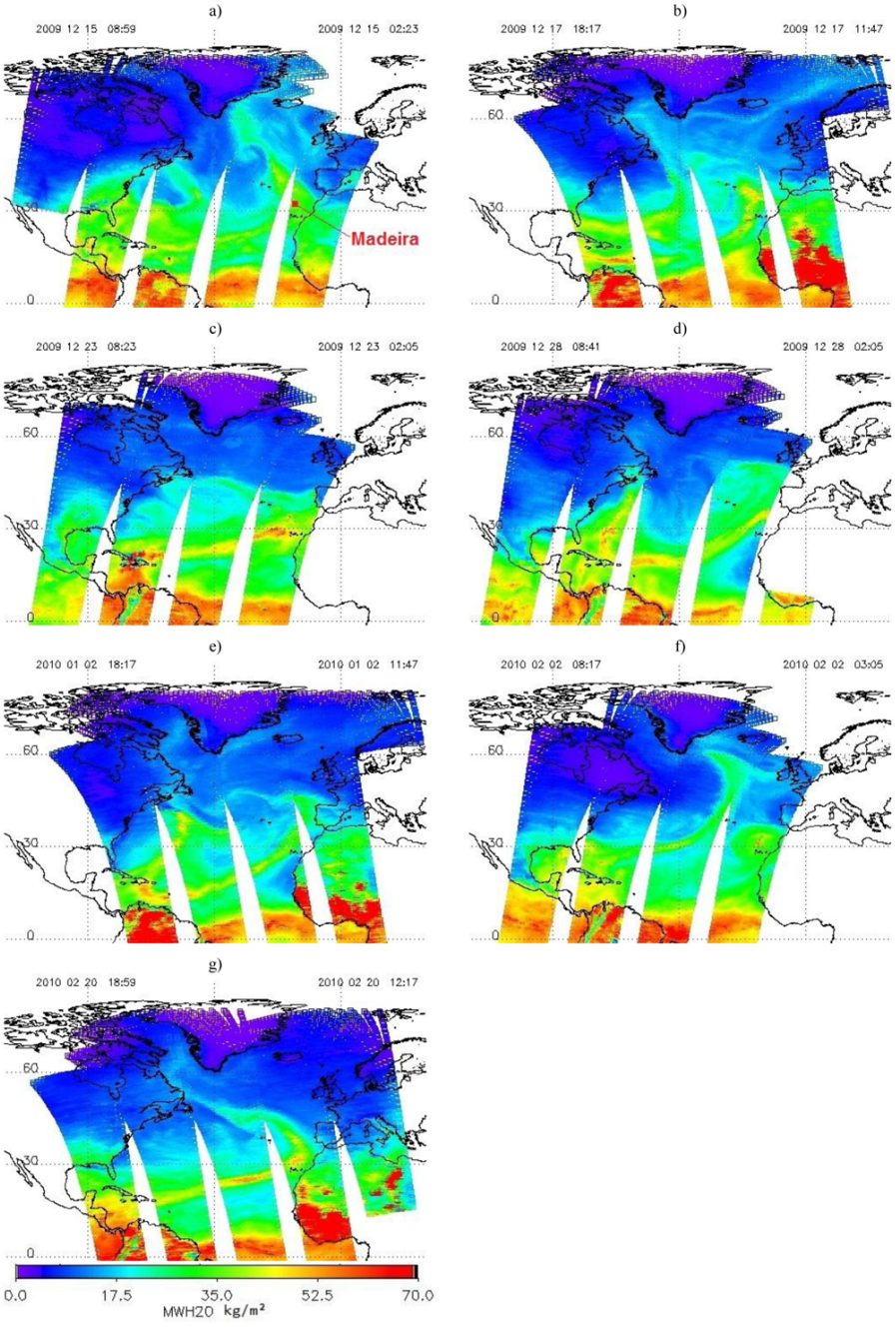

Fig. 4. Satellite images of precipitable water obtained from the Atmospheric InfraRed Sounder (Aqua-AIRS) for each case study. **(a)** 15 December 2009, **(b)** 17 December 2009, **(c)** 23 December 2009, **(d)** 28 December 2009, **(e)** 2 January 2010, **(f)** 2 February 2010, and **(g)** 20 February 2010.

3.2 Numerical simulations and mesoscale analysis

In this section, the simulation results obtained for four of the cases are presented, aiming at finding other aspects related to the high precipitation amounts rather than only synoptic similarities. The cases simulated correspond to the following days: 22 December 2009 (CASE 1), 28 December 2009 (CASE 2), 2 February 2010 (CASE 3), and 20 February 2010 (CASE 4), also listed in Table 2.

3.2.1 Model validation

One of the well known problems related to grid-spacing decrease is associated with slight displacement errors, which

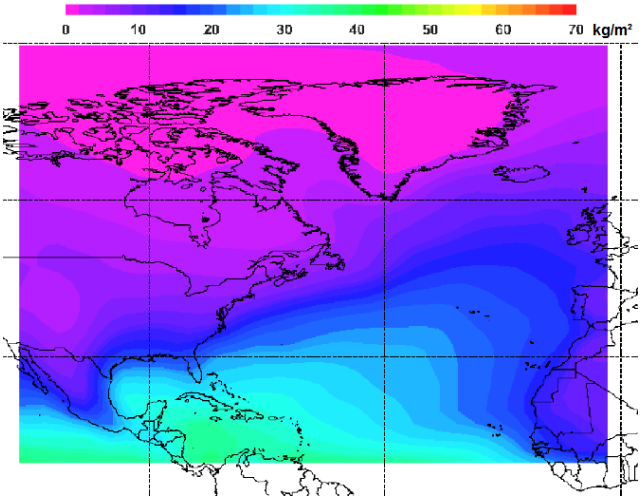

Fig. 5. Average value of the total precipitable water over thirty years (1979–2009) obtained for the month of February from the NCEP/DOE AMIP-II Reanalysis (Reanalysis-2).

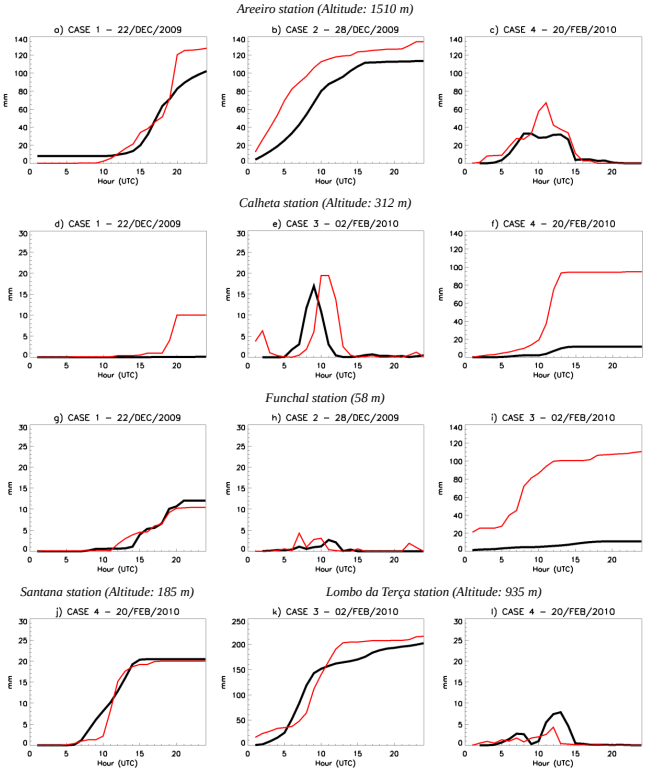

Fig. 6. Comparison between the temporal evolution of hourly precipitation (HP) and accumulated precipitation (AP), both measured (red) and simulated (black) for: Areeiro station **(a)** AP on 22 December, **(b)** AP on 28 December, **(c)** HP on 20 February; Calheta station **(d)** AP on 22 December, **(e)** HP on 02 February, **(f)** AP on 20 February; Funchal station **(g)** AP on 22 December, **(h)** HP on 28 December, **(i)** AP on 02 February; Santana station **(j)** AP on 20 February; Lombo da Terça **(k)** AP on 02 February, and **(l)** HP on 20 February.

often result in double penalties, creating difficulties to assess the true quality of high resolution simulations (Clark et al., 2010). Many studies have been focused on the verification practices; for example, Casati et al. (2008) presented a review of the forecast verification procedures, related to spatial verification methods, probabilistic forecasts and ensemble verification. Despite the limitations of standard verification methods based on a point by point comparison, these have been used to evaluate the performance of the MESO-NH model, essentially for accumulated and hourly precipitation. For each meteorological station (see Table 1), a modeled value was selected from the four closest grid-points, corresponding to the smallest difference between simulation results and observations. The results of the comparison between observed and simulated precipitation values are presented in Fig. 6 for a selection of some representative plots regarding the inner model performance evaluation. For Areeiro station, located near the summit of the mountain (Fig. 6a, b, and c), the model satisfactorily represented the temporal evolution of rainfall in the three simulations, despite some underestimation of the accumulated precipitation in all cases.

In the case of Calheta station, the model did not accurately simulate the precipitation, at least in the 22 December event (Fig. 6d) and in the most intense event (Fig. 6f). However, for 02 February (Fig. 6e), the model exhibited a good temporal evolution of the hourly precipitation, with similar maximum intensities and small phase differences. At lower altitudes, for example at Funchal station, both for 22 December (Fig. 6g) and 28 December (Fig. 6h), the precipitation was well represented by the model, even though the model slightly overestimated the observed rainfall during 22 December. However, for 02 February (Fig. 6i), the precipitation was poorly represented by the model, which underestimated the precipitation by approximately 100 mm. On the other hand, in the 20 February case, the model also represented the precipitation behavior at low levels well, as shown in Fig. 6j for Santana station. Nevertheless, the general analysis of the results shows that the model presented the best results for the stations located on high levels of the island, as well as for the two most intense cases, 20 February and 02 February. These aspects are confirmed not only by the comparison between observed and simulated precipitation at Areeiro station, but also at Lombo da Terça station, where good results were obtained for the simulated precipitation, such as verified on 2 February (Fig. 6k) and 20 February (Fig. 6l).

This simple comparison was not made in order to quantify the quality of the precipitation forecast, but rather to verify if the model is able to properly capture the events of intense precipitation. The success of the model in simulating the accumulated precipitation, especially in the regions where the maximum values were recorded, indicates that it can be used

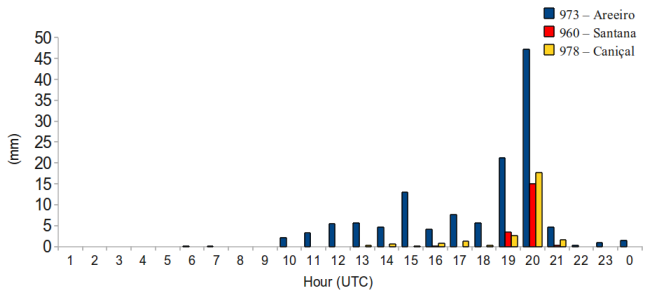

Fig. 7. Diurnal variations of total hourly rainfall (mm) for Areeiro, Santana, and Caniçal station, on 22 December 2009.

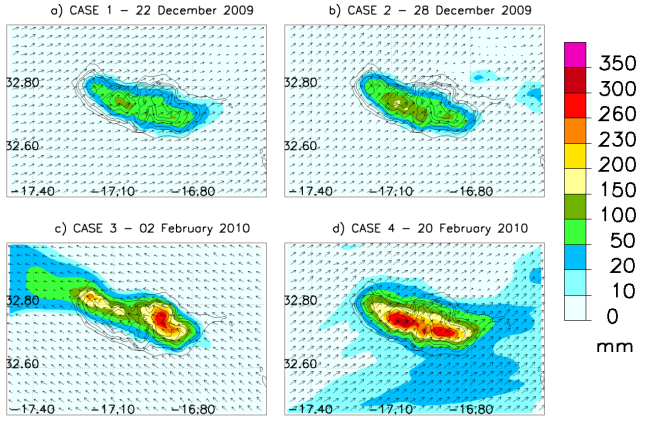

Fig. 8. The shaded areas represent the daily accumulated precipitation (mm) simulated with the MESO-NH model, solid lines represent the Madeira orography (m) obtained from the GTOPO30 database, and arrows represent the horizontal wind vectors at model level 18, approximately 1 km above the surface: **(a)** 22 December 2009 and wind vectors at 20:00 UTC, **(b)** 28 December 2009 and wind vectors at 05:00 UTC, **(c)** 2 February 2010 and wind vectors at 07:00 UTC, and **(d)** 20 February 2010 and wind vectors at 12:00 UTC.

to improve our understanding in relation to the mechanisms responsible for its occurrence.

3.2.2 Rainfall behavior

Figure 7 shows the distribution of the observed hourly precipitation at the surface stations for CASE 1. It can be observed that the largest accumulated values occurred in the late afternoon and early evening, around 20:00 UTC. However, at Areeiro station, there was precipitation since 10:00 UTC, which intensified throughout the afternoon, reaching an hourly maximum value of 47.3 mm at 20:00 UTC. At the other stations, the maxima were also observed around 20:00 UTC, but with values lower than those observed in Areeiro, with maxima of 17.7 mm at Caniçal station and 15 mm at Santana station (Fig. 7). Therefore, the highest value of accumulated precipitation in 24 h was registered at Areeiro station (127.7 mm).

Figure 8 shows the horizontal wind vectors at approximately 1 km altitude for each case when the maximum rainfall was recorded, as well as the daily accumulated precipitation (24 h) produced by the high resolution inner model. It is possible to identify from the wind field a southwestern flow in three of the four cases (CASE 1 – Fig. 8a, CASE 2 – Fig. 8b, CASE 4 – Fig. 8d), agreeing with the large-scale analysis (see Sect. 3.1), where the presence of atmospheric rivers, flowing from southwest and acting over Madeira, was identified.

From the daily accumulated precipitation for CASE 1 (Fig. 8a), it is possible to observe that the precipitation was located mainly over the island, while over the ocean the daily accumulated precipitation was about 10 mm. In the same figure it may be verified that the highest values of accumulated precipitation (between 100 mm and 150 mm) are obtained over the central part of the island, localized mainly in the Paúl da Serra region (above 1000 m) and in a less extensive area over the Areeiro peak (above 1500 m).

Similarly to CASE 1, the observed precipitation in CASE 2 (not shown) indicates that the greatest records of hourly precipitation were also collected at Areeiro. In this case, precipitation intensities greater than 10 mm h^{-1} were recorded between 01:00 UTC and 06:00 UTC, with a peak of 16.1 mm h^{-1} at 05:00 UTC. Nevertheless, the rain remained weak throughout the day, with another maximum after 22:00 UTC, but still lower than 5 mm, with a total of 135.1 mm of accumulated daily precipitation. The high resolution simulation was able to show that the accumulated precipitation maxima occurred in the highest regions of the island, with values between 150 mm and 200 mm in Paúl da Serra and between 100 mm and 150 mm at Areeiro Peak. Over the ocean, on the northeastern coast, a small region with rainfall between 10 and 50 mm can be identified (Fig. 8b). This precipitation may be caused by a specific orographic mechanism, lee-side triggering of convection (cf. Houze, 1993), since the block caused by the island forces the wind around, subsequently converging in low levels. According to the present study, in the case of Madeira this mechanism does not seem to be very relevant since it occurs over the ocean, but in other regions of the globe it can be a very important mechanism triggering deep convection and consequently associated with severe weather conditions. Therefore, in CASE 2, the high rainfall amount over land is related to different mechanisms of orographic precipitation. In the early morning, the upslope condensation appears to be the dominant mechanism, favoring stratiform rainfall for many hours. In contrast, in the evening the orographic lifting was responsible for the development of localized rainfall not significant at the scale of the island.

Figure 8c illustrates the daily accumulated precipitation over Madeira island obtained in the simulation of CASE 3, the second most intense case. CASE 3 is marked

by high daily accumulated precipitation values recorded at some meteorological stations: Funchal (110.7 mm), Santana (108 mm), Areeiro (273.1 mm), Lombo da Terça (216.1 mm). Maximum hourly accumulated values were observed at Santana (35.3 mm at 04:00 UTC) and at Areeiro (29.2 mm at 11:00 UTC). Weak precipitation also occurred during the afternoon, and later at 23:00 UTC another hourly relative maximum was recorded at Areeiro station (11.5 mm). In the 1 km simulation, the greatest values were obtained in Madeira's highlands, with an accumulated precipitation between 260 mm and 300 mm (Fig. 8c). In this case, a large-scale forcing was present, favoring the establishment of the orographic precipitation mechanism known as seeder-feeder. The precipitation was generated from the clouds that formed over the island and increased due to rainfall from higher clouds associated with the low pressure system, also contributing to trigger convection.

The fourth and most intense simulated event corresponds to the disaster that occurred on 20 February 2010 (CASE 4). The disaster caused more than 40 deaths, many people missing and wounded, as well as a vast range of material losses, including the destruction of houses, industries, roads, bridges and several thousands of vehicles. This situation was observed mainly in the southern regions of the island. Many of the surface stations presented defects or were definitely wrecked due to landslides or even the high rainfall amounts, and they did not register any rainfall during the afternoon. Nevertheless, the highest values of hourly accumulated precipitation (not shown) were observed at 11:00 UTC at Areeiro station (67 mm), at 12:00 UTC at Calheta (38.1 mm), at 08:00 UTC at Ponta do Sol (28.2 mm), at 09:00 UTC at Funchal (51.2 mm), and at 10:00 UTC at Caniçal station (21.3 mm). As for the daily accumulated precipitation, the observation records give: 144.3 mm (Funchal station), 387.1 mm (Areeiro station), 95.3 mm (Ponta do Sol) and 94.7 mm (Calheta station). Figure 8d shows the results of the modeled accumulated precipitation corresponding to CASE 4. It can be noted that the model simulates the greatest accumulated records over the island, indicating the important effect of orography on the intensification of precipitation, given the large differences between the rainfall amounts over the island and over the ocean. In this case, the precipitation observed over the ocean was caused mainly by the passage of the frontal system. In addition to the orographic effects, the precipitation observed over the island was intensified by the seeder-feeder mechanism, with rainfall in low levels being increased by precipitation originated in higher frontal clouds.

The accumulated precipitation simulated by the model, which was running in prognostic mode for this case, is presented in Fig. 9. The results show that the model simulates the accumulated rainfall and the orographic effect on the precipitation enhancement well. In general, the results are close to those obtained in diagnostic mode (see Fig. 8d), with the areas of greatest records found over the island in the highlands and not exceeding 311 mm. This simulation confirms the ability of the MESO-NH model to predict these high precipitation events.

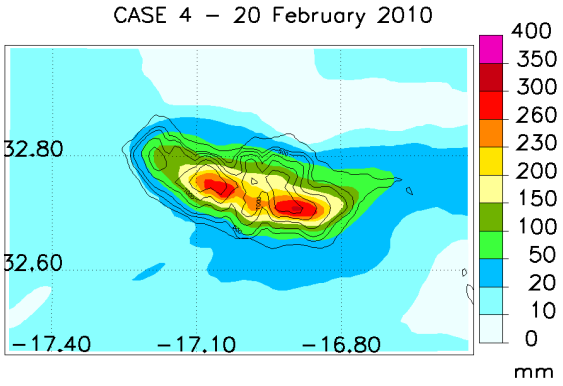

Fig. 9. Forecast of accumulated precipitation for 20 February 2010 is represented by the shaded areas, while the solid lines represent Madeira orography (m). The orography is simulated from GTOPO30 database with 1 km resolution.

3.2.3 Atmospheric stability

The atmospheric stability is evaluated in terms of the simulated Convective Available Potential Energy – CAPE. In the first case, i.e. 22 December 2009, the model simulates low CAPE values during the morning and early afternoon, with values that do not exceed 250 J kg^{-1} at 12:00 UTC (Fig. 10a). After 18:00 UTC there was a slight increase of instability, since CAPE values are greater than 500 J kg^{-1} in all regions except over the island, where the values are below 150 J kg^{-1} (figure not shown here). However, a region of moderately unstable air was found at 20:00 UTC to the southwest coast of the island (Fig. 10b), with CAPE between 1000 J kg^{-1} and 1250 J kg^{-1} over the ocean, favoring a possible trigger of convection.

In contrast to CASE 1, in the second case (CASE 2, 28 December 2009) the simulated CAPE indicates a marginally unstable atmosphere throughout the day. Figures 10c and d illustrate this feature both at 05:00 UTC and at 23:00 UTC, when other low rainfall maxima were identified. The mountain effects (e.g. foehn effect) on this variable can be clearly distinguished: over the south/southwestern regions off the island coast the CAPE values vary between 500 and 1000 J kg^{-1}, while over the north/northeastern sections the values are lower, between 0 and 500 J kg^{-1}.

For the second most intense event (CASE 3, 2 February 2010), based on the model results, low CAPE values are also obtained from the simulations during the day, both over the island and adjacent oceanic regions. Areas of CAPE between 200 and 500 J kg^{-1} are identified mainly around the island over the ocean, while values between 25 and 200 J kg^{-1} in the central and western regions of the island (Fig. 10e), confirm that other factors were necessary in order to trigger

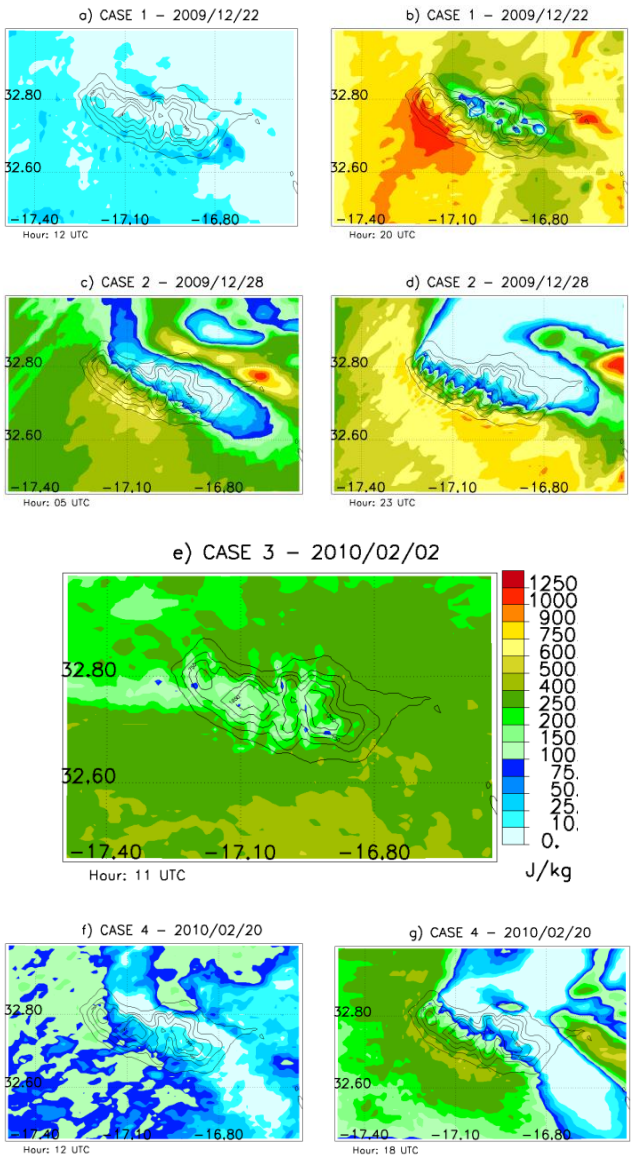

Fig. 10. Convective Available Potential Energy ($J\,kg^{-1}$) simulated with the MESO-NH Model for **(a)** 22 December 2009 – 12:00 UTC, **(b)** 22 December 2009 – 20:00 UTC, **(c)** 28 December 2009 – 05:00 UTC, **(d)** 28 December 2009 – 23:00 UTC, **(e)** 2 February 2010 – 11:00 UTC, **(f)** 20 February 2010 – 12:00 UTC, and **(g)** 20 February 2010 – 18:00 UTC.

convection, since an atmosphere with weakly unstable conditions was identified. At the end of the day, CAPE values larger than $250\,J\,kg^{-1}$ were not found over the island and adjacent ocean (figure not shown here).

In CASE 4, the most intense case, a marginally unstable atmosphere was also found. As seen in Fig. 10f, the CAPE values at 12:00 UTC do not exceed $200\,J\,kg^{-1}$. In the afternoon, there is an increase of instability, but CAPE does not exceed $750\,J\,kg^{-1}$, still indicating a weakly unstable atmosphere (Fig. 10g). Therefore, the simulations indicate that high CAPE values appear not to be a necessary condition for the occurrence of high rainfall events on Madeira Island, since low values were found in most of the cases.

In general, the results of the simulations showed that the 2009/2010 high rainfall amounts and flooding on Madeira occur in a stable, marginally or moderately unstable atmosphere. According to the simulations, none of the high precipitation events were associated with very or extremely unstable conditions.

3.2.4 Vertical motion

The results obtained in the last subsection regarding the atmospheric stability point out that the orography-induced vertical motion over the island may be an important factor in the development of cloudiness and a possible trigger of convection, since a marginally unstable atmosphere was identified in most of the cases. In order to analyze this hypothesis, the simulated vertical velocity at some time steps is presented in this section, considering both horizontal levels and vertical cross-sections. The vertical cross-sections shown in Figs. 11 and 12, different for each case, were selected in order to highlight some of the most interesting features.

From the simulations for 22 December 2009 (CASE 1), positive nuclei (upward motion) were found in the south/southwestern part of the island. These regions are favored by the large-scale southwestern low level flow with the presence of an atmospheric river structure, as identified in Sect. 4.1 and Fig. 8a. From the vertical cross-section shown in Fig. 11a, it is possible to identify over the Areeiro peak a nucleus with positive vertical velocity, extending from the surface up to approximately 4 km, around the time when the rainfall maxima were recorded. The maximum values are observed between 1.5–3.5 km altitude and are sometimes larger than $10\,m\,s^{-1}$.

During the second case study (28 December 2009), when the maximum rainfall occurred in the early morning, the upward motion was generated mainly in the south/southwestern part of the island favored by the southwestern low level flow, which was a predominant large-scale feature throughout the day (see Fig. 8b). The simulation at 05:00 UTC (Fig. 11b) shows the regions of upward motion, which can be identified in the lower levels over the island, but the magnitude is lower than in CASE 1, with nuclei of about $3\,m\,s^{-1}$ up to an altitude of 1.5 km over the Areeiro peak. Above this level the upward motion does not exceed $1\,m\,s^{-1}$ (Fig. 11b).

In CASE 3 (2 February 2010), the southeastern flow identified at lower levels during the morning (Fig. 8c) favors the formation of an anabatic upward motion over the island, particularly on its east coast (Fig. 11c), with intensities greater than $4.4\,m\,s^{-1}$ and a maximum above $8.0\,m\,s^{-1}$. From the vertical cross-section, upward motions are identified through the troposphere up to 10 km of altitude over the highest regions of the island, which are an indication of the occurrence

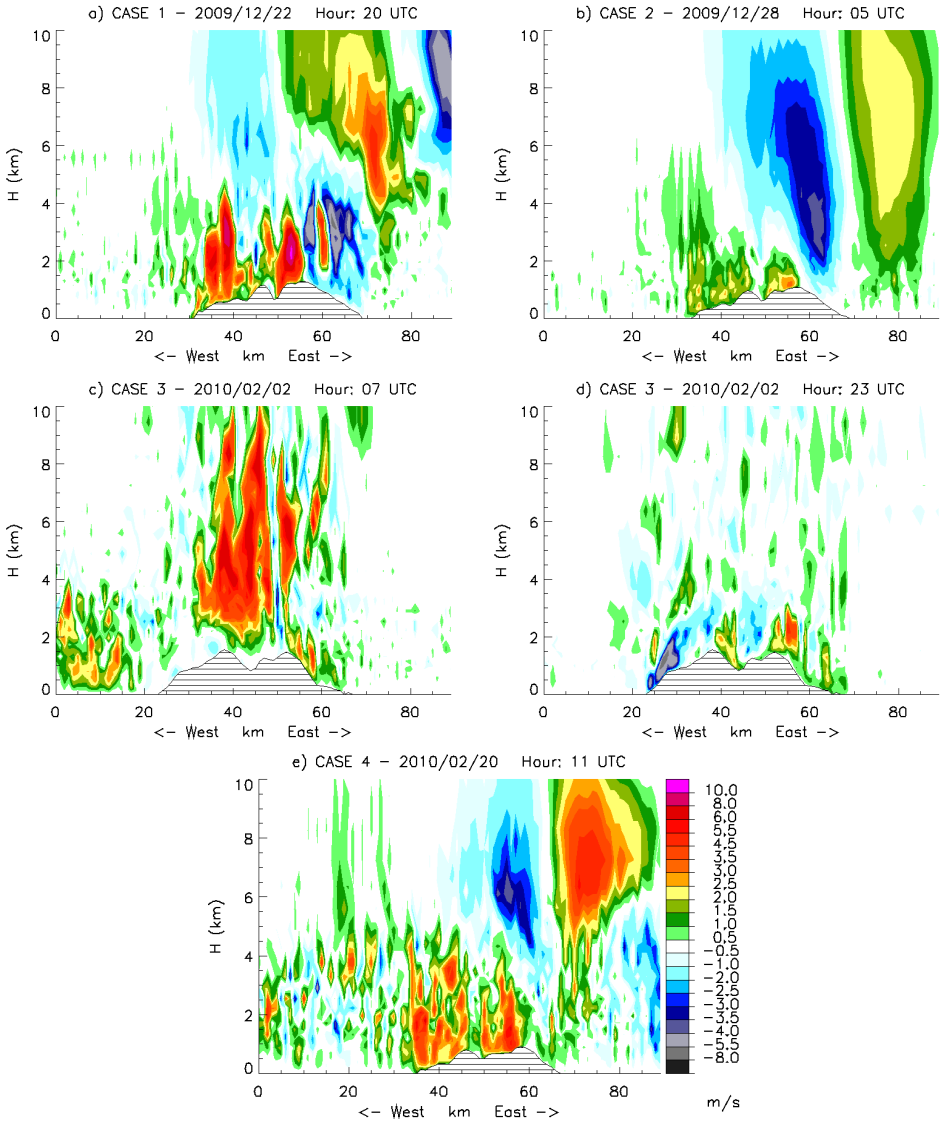

Fig. 11. Vertical east–west cross-section of the vertical velocity ($m\,s^{-1}$) simulated with MESO-NH for **(a)** 22 December 2009 – 20:00 UTC and cross-section in $y = 27.7$; **(b)** 28 December 2009 – 05:00 UTC and cross-section in $y = 26$; **(c)** 2 February 2010 – 07:00 UTC and cross-section in $y = 34$; **(d)** 2 February 2010 – 23:00 UTC and cross-section in $y = 34$; and **(e)** 20 February 2010 – 11:00 UTC and cross-section in $y = 25$.

of deep convection. The nuclei of intense positive vertical velocity were identified at medium levels with velocities between 6 and 8 $m\,s^{-1}$. At 23:00 UTC (Fig. 11d), in the eastern part of the island, upward motion with velocities greater than 3 $m\,s^{-1}$ is identified in approximately 2–3 km altitude and influenced basically by the steep orography of the island.

Lastly, in CASE 4 (20 February 2010), the positive vertical motion regions that occurred on the south/southwest coast of the island were favored by a southwestern flow at low levels (see Fig. 8d), which encompasses the presence of an atmospheric river, such as in CASE 1 and CASE 2. At the 850 hPa level, the velocities range between 2.3 $m\,s^{-1}$ and 6 $m\,s^{-1}$ (850 hPa), in contrast with the medium level, where the model does not generate intense vertical velocities, these being lower than 2 $m\,s^{-1}$ (figures not shown here). Figure 11e represents the vertical east–west cross-section of the vertical velocity at 11:00 UTC, and regions of upward motion are clearly identified over the island, mainly influenced by orography. However, over the Areeiro peak, the upward motions are more intense, with velocities greater than 5 $m\,s^{-1}$ near the surface, although this intense vertical velocity region does not exceed 4 km altitude.

In the simulated cases, the steep orography was the main factor in creating and intensifying the upward motions (positive vertical velocities), since the maximum values were simulated over the island and in most cases at lower levels.

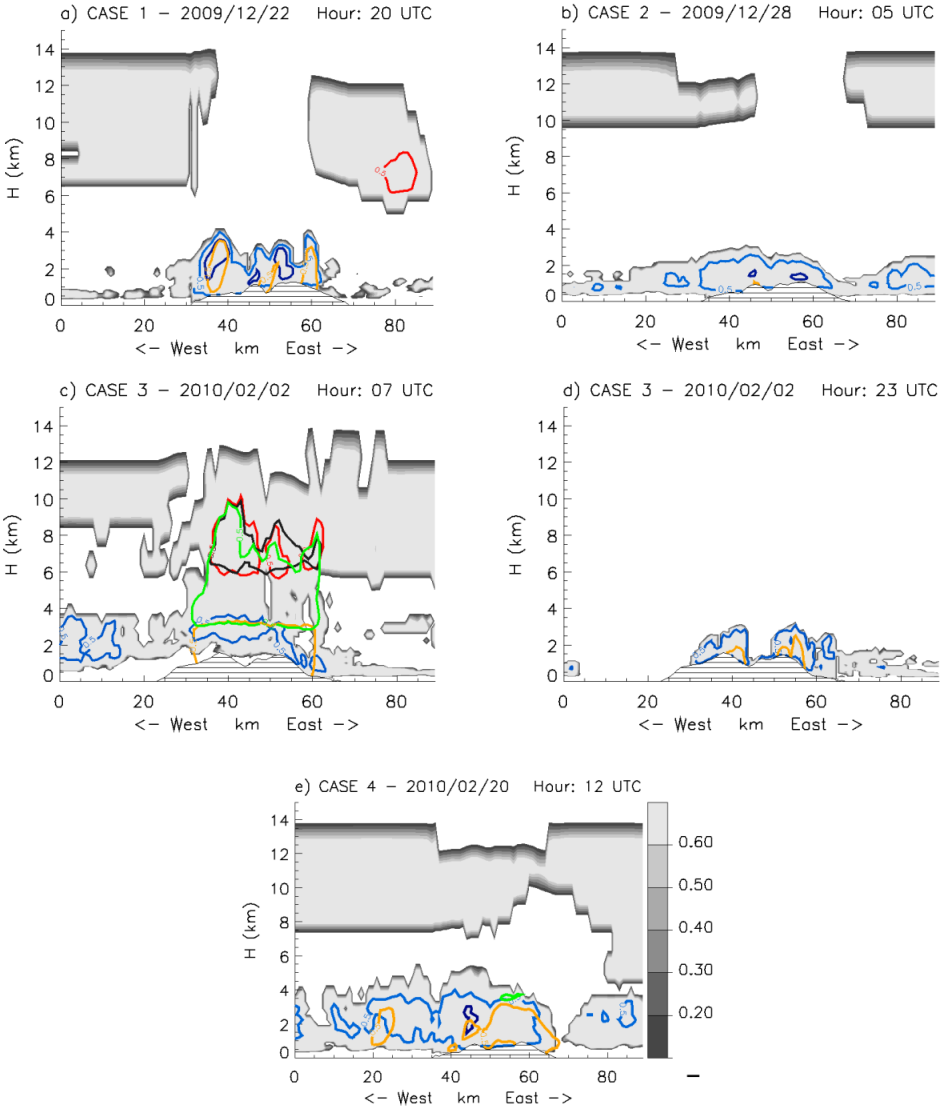

Fig. 12. Vertical cross-section of mixing ratio simulations for cloud water (MRC; blue lines of 0.5 g kg^{-1} and dark blue lines of 1.5 g kg^{-1}), rain (MRR; yellow lines of 0.5 g kg^{-1}), ice (MRI; red lines of 0.5 g kg^{-1}), snow (MRS; black lines of 0.5 g kg^{-1}) and graupel (MRG; green lines of 0.5 g kg^{-1}), as well as the cloud fraction (shaded areas). **(a)** 22 December 2009 – at 20:00 UTC and cross-section in $y = 27.7$; **(b)** 28 December 2009 – at 05:00 UTC and cross-section in $y = 26$; **(c)** 2 February 2010 – at 07:00 UTC and cross-section in $y = 34$; **(d)** 2 February 2010 – at 23:00 UTC and cross-section in $y = 34$; and **(e)** 20 February 2010 – at 12:00 UTC and cross-section in $y = 25$.

The presence of downdraft nuclei is evident in all cases, and their locations depend on the island orientation in relation to the low level mean flow. The existence of these downdrafts gives rise to zones with relatively lower rainfall amounts, contributing to the complex pattern of the simulated precipitation field.

3.2.5 Hydrometeor distributions

Since one of the goals of this work is the understanding of some of the aspects related to the increase of rainfall amounts in Madeira's highlands on the basis of the parameters examined above, the model output of the mixing ratio for cloud water (MRC), rain (MRR), ice (MRI), snow (MRS) and graupel (MRG), as well as the cloud fraction, are shown and analyzed.

As already mentioned, the precipitation observed on 22 December 2009 in Madeira's highlands started weakly and continuously, mainly due to the weakly unstable anabatic flow created by the presence of the island. The presence of low clouds over the island at 12:00 UTC (figure not shown here), visible in the simulated cloud fraction, contributes to this assumption. As for the vertical distribution of the hydrometeors, regions with MRC of about

$1\,g\,kg^{-1}$ were simulated at 12:00 UTC over the island, which intensify during the afternoon. At 20:00 UTC (blue lines; Fig. 12a), the simulation produced values of about $0.5\,g\,kg^{-1}$ and $1.5\,g\,kg^{-1}$ (dark blue lines) in the highest points of the island. These large MRC values together with MRR values of $0.5\,g\,kg^{-1}$ (yellow lines) confirm that the most intense precipitation (between 19:00 and 20:00 UTC) occurred basically from the formation of dense clouds near the surface, since these clouds do not exceed 4 km altitude. However, in the same figure, high clouds (above 6 km altitude) are present in the model, as observed in the cloud fraction field (shaded areas).

In CASE 2, a persistent cloudiness was identified at low levels, but not exceeding 3 km altitude at 05:00 UTC. However, the model indicates that the orographic lifting induces condensation over the island, since the maximum values of MRC appeared over the Areeiro peak, with intensities of roughly $1.5\,g\,kg^{-1}$ and not exceeding 2 km altitude (dark blue lines; Fig. 12b). On the other hand, over the western peak of the island, values between $1.5\,g\,kg^{-1}$ and $2\,g\,kg^{-1}$ were simulated during the morning and early afternoon, not exceeding 2.5 km altitude (figures not shown here). The absence of atmospheric ice over the island and the cloud fraction pattern both indicate the presence of clouds with weak vertical development; however, high clouds can also be seen from the results.

In general, during the morning of 2 February (CASE 3), intense upward motions were modeled over the island, as shown in the vertical velocity analysis. High values of MRC have been identified, with values of about $0.5\,g\,kg^{-1}$ (at 07:00 UTC) at approximately 3 km altitude (blue lines; Fig. 12c), and $1.5\,g\,kg^{-1}$ at 09:00 UTC (figures not shown here). Significant values were observed near the surface at the eastern peak of the island, with MRR values above $0.5\,g\,kg^{-1}$ (yellow lines). The presence of MRI values above $0.5\,g\,kg^{-1}$ (red lines) in the middle troposphere, together with significant values of MRS (black lines; about $0.5\,g\,kg^{-1}$) and MRG (green lines; values above $0.5\,g\,kg^{-1}$), indicate the occurrence of deep convection in this case. Therefore, the simulated cloud fraction (Fig. 12c) suggests the presence of the seeder-feeder mechanism acting to intensify the preexistent precipitation at low levels. In addition, convective trigger occurred, since the model indicates that the clouds extend from the surface of the island to approximately 12 km altitude mainly during the early morning. This assumption is based on the intense upward motion, as already verified, as well as the high amounts of cloud water at low levels followed above by an intense area of several hydrometeors.

Purely orographic clouds over Madeira were observed during the end of the day, when another maximum of precipitation was recorded. The cloud fraction vertical cross-section at 23:00 UTC shows that the orographic lifting was the main factor acting in the intensification of the condensation process over the highest regions of the island. This is confirmed by the absence of high clouds and of significant values of mixing ratio for other hydrometeors. Significant values of cloud water mixing ratio (blue lines; values above $0.5\,g\,kg^{-1}$) up to 3 km height were also obtained from the simulation (Fig. 12d). Values of the same magnitude were also observed for rain water mixing ratio (yellow lines).

In CASE 4, Fig. 12e shows a vertical cross-section of cloud fraction at 12:00 UTC, where it is possible to observe the presence of high clouds above 7.5 km altitude as well as of a dense layer of cloudiness at low levels, especially over the island, reaching approximately 5 km altitude. Once again, the simulated field of MRC indicates the effect of the orography on intensifying the condensation processes over the island, where the larger amount of mixing ratio was found, with values above $0.5\,g\,kg^{-1}$ over the island and ocean, as well as values larger than $1.5\,g\,kg^{-1}$ in the western peak (dark blue lines). The simulation shows high values from the surface up to 5 km, indicating the presence of dense low and medium level cloudiness. Significant values are identified for MRR (yellow lines) and MRG (green lines) with maximum magnitudes of $0.5\,g\,kg^{-1}$. Therefore, in the most intense case, the passage of a frontal system, preceded by the action of the atmospheric river at low levels, acted to intensify the process of precipitation on the island. On the other hand, the seeder-feeder mechanism could be identified once more, as the precipitation of medium and high clouds appears to contribute to the intensification of precipitation of the purely orographic lower clouds. Thus, local conditions, such as the local steep orography and high amounts of moisture at low levels, once more were crucial to the development of high amounts of rainfall. In this case it was sufficient to cause the catastrophe observed on this day (20 February 2010).

4 Conclusions

The main atmospheric characteristics associated with episodes of high rainfall that occurred during the winter of 2009/2010 on the highlands of Madeira Island have been investigated in this study. Precipitable water from satellite observations, as well as synoptic charts have been analyzed for the seven cases. In addition, high resolution simulations were run and used to analyze the four most intense cases. Although the study of only seven cases, four of them modeled, may not be sufficient to draw definitive conclusions about heavy rainfall episodes on Madeira Island, the study is deemed useful to highlight some important aspects that were observed throughout the development of this work.

The orography of Madeira is the dominant factor both in the formation and intensification of precipitation, inferred in all simulated cases from the differences between daily rainfall amounts over the island and over the adjacent ocean, sometimes with differences greater than 100 mm. Over the island, the altitude is the main factor contributing to the precipitation distribution, the highest records being verified in the highlands, contrasting with the lowest values in regions

at lower altitude. This feature was observed from rain gauge data and represented in the simulations. On the other hand, the precipitation in the lower regions of the island has a spatial variation depending on the flow direction at low levels and, consequently, on the synoptic pattern observed.

The formation of clouds with thicknesses of a few kilometers indicates that the anabatic flow created by the presence of the island is sufficient to induce the development of dense clouds and events of high precipitation, even in marginally unstable conditions (CAPE lower than $1000\,\mathrm{J\,kg^{-1}}$), provided that the low level atmospheric moisture is sufficiently high. Only one of the cases studied shows a moderately unstable atmosphere, while in all other cases the simulated CAPE indicates stable or marginally unstable conditions, which do not favor the triggering of deep convection. Therefore, intense precipitation events on Madeira are not necessarily associated with thermodynamic instability, the orographic effect allied to high precipitable water values being the crucial factor to generate these occurrences.

Two types of synoptic systems were identified during the days of maximum rainfall on Madeira. In six out of the seven cases analyzed, the passage of a cold front and the presence of atmospheric rivers, acting to increase moisture in the lower atmospheric levels, together with the orographic lifting induced the heavy precipitation events. In the remaining case the synoptic situation is characterized by the presence of a low pressure system centered between the Madeira Archipelago and the Canary Islands. In general, the transport of water vapor from the tropics towards higher latitudes, representing the tropical–extratropical interaction, has been considered the main factor to favor the increase of the orographic rainfall amounts over the island.

The MESO-NH model has satisfactorily reproduced the main features related to the four simulated cases, taking into account the known difficulties related to the comparison between local precipitation observations and high resolution simulation results in mountainous regions. The efficiency of MESO-NH in predicting heavy rainfall over Madeira was proven by the simulation for the most intense case (20 February 2010), confirming the fact that it is possible to obtain good forecasts of rainfall for Madeira island, based on atmospheric models with high horizontal resolution ($\sim$1 km). Knowing that the atmospheric rivers are responsible for much of the water vapor transport from the tropics towards higher latitudes, and that they were present in six of the seven cases analyzed, the use of atmospheric precipitable water amounts obtained from satellites can be a valuable aid in the prediction and early warning of extreme precipitation events on Madeira.

In summary, through the development of this work, it is concluded that the high rainfall amounts observed during the winter of 2009/2010 on Madeira Island were directly related to the orographic forcing. In most of the selected cases, the lifting occurs with the most intense vertical velocities mainly over the island and near the surface, not exceeding the middle levels. However, the development of precipitation over the island can be intensified by large-scale patterns, such as the passage of weather systems like fronts or low pressures. For example, the atmospheric river structures associated with frontal systems act to provide the necessary moisture conditions for the intensification of orographic precipitation. Southwestern winds at low levels favor the transport of moisture to the upper regions of the island, contributing to the formation of denser clouds, although with weak vertical development.

Acknowledgements. The authors would like to acknowledge the AIRS Science Team for the development of the AIRS Products and the Portuguese Instituto de Meteorologia, which provided the surface data and synoptic charts.

This work was co-financed through FEDER (Programa Operacional Factores de Competitividade – COMPETE) and National funding through FCT – Fundação para a Ciência e a Tecnologia in the framework of projects FCOMP-01-0124-FEDER-007122 (PTDC/CTE-ATM/65307/2006) and FCOMP-01-0124-FEDER-009303 (PTDC/CTE-ATM/102142/2008).

Edited by: A. Mugnai
Reviewed by: two anonymous referees

References

Aumann, H. H., Chahine, M. T., Gautier, C., Goldberg, M., Kalnay, E., McMillin, L., Revercomb, H., Rosenkranz, P. W., Smith, W. L., Staelin, D. H., Strow, L., and Susskind, J.: AIRS/AMSU/HSB on the Aqua Mission: Design, Science Objectives, Data Products and Processing Systems, IEEE T. Geosci. Remote, 41, 253–264, 2003.

Barthlott, C., Burton, R., Kirshbaum, D., Hanley, K., Richard, E., Chaboureau, J.-P., Trentmann, J., Kern, B., Bauer, H.-S., Schwitalla, T., Keil, C., Seity, Y., Gadian, A., Blyth, A., Mobbs, S., Flamant, C., and Handwerker, J.: Initiation of deep convection at marginal instability in an ensemble of mesoscale models: A case-study from COPS, Q. J. Roy. Meteor. Soc., 137, 118–136, 2011.

Bechtold, P., Bazile, E., Guichard, F., Mascart, P., and Richard, E.: A mass flux convection scheme for regional and global models, Q. J. Roy. Meteor. Soc., 127, 869–886, 2001.

Bergeron, T.: Über den Mechanismus der ausgiebigen Niederschläge, Ber. Deut. Wetterd., 12, 225–232, 1950.

Bergeron, T.: On the low-level redistribution of atmospheric water caused by orography, Proceedings, International Cloud Physics Conference, Toronto, 1968.

Borges, P. A. V., Abreu, C., Aguiar, A. M. F., Carvalho, P., Fontinha, S., Jardim, R., Melo, I., Oliveira, P., Sequeira, M. M., Sérgio, C., Serrano, A. R. M., Sim-Sim, M., and Vieira, P.: Terrestrial and freshwater biodiversity of the Madeira and Selvagens archipelagos, in: A list of the terrestrial fungi, flora and fauna of Madeira and Selvagens archipelagos, edited by: Borges, P. A. V., Abreu, C., Aguiar, A. M. F., Carvalho, P., Jardim, R., Melo, I., Oliveira, P., Sérgio, C., Serrano, A. R. M., and Vieira, P.,

Direcção Regional do Ambiente da Madeira and Universidade dos Açores, Funchal and Angra do Heroísmo, 13–26, 2008.

Bougeault, P. and Lacarrère, P.: Parameterization of orography-induced turbulence in a meso-beta scale model, Mon. Weather Rev., 117, 1872–1890, 1989.

Bougeault, P., Binder, P., Buzzi, A., Dirks, R., Houze, R., Kuettner, J., Smith, R. B., Steinacker, R., and Volkert, H.: The MAP Special Observing Period., B. Am. Meteorol. Soc., 82, 433–462, 2001.

Carlson, T. N.: Mid-latitude Weather Systems, Harper Collins Academic, 507 pp., 1991.

Caroletti, G. N. and Barstad, I.: An assessment of future extreme precipitation in western Norway using a linear model, Hydrol. Earth Syst. Sci., 14, 2329–2341, doi:10.5194/hess-14-2329-2010, 2010.

Casati, B., Wilson, L. J., Stephenson, D. B., Nurmi, P., Ghelli, A., Pocernich, M., Damrath, U., Ebert, E. E., Brown, B. G., and Mason, S.: Forecast verification: current status and future directions, Meteorol. Appl., 15, 3–18, doi:10.1002/met.52, 2008.

Chu, P.-S., Zhao, X., Ruan, Y., and Grubbs, M.: Extreme rainfall events in the Hawaiian Islands, J. Appl. Meteorol. Clim., 48, 502–516, doi:10.1175/2008JAMC1829.1, 2009.

Chu, P.-S., Chen, Y. R., and Schroeder, T. A.: Changes in precipitation extremes in the Hawaiian Islands in a warming climate, J. Climate, 23, 4881–4900, doi:10.1175/2010JCLI3484.1, 2010.

Clark, A. J., Gallus, W. A., and Weisman, M. L.: Neighborhood-based verification of precipitation forecasts from convection-allowing NCAR WRF model simulations and the operational NAM, Weather Forecast., 25, 1495–1509, doi:10.1175/2010WAF2222404.1, 2010.

Costa, M. J., Salgado, R., Santos, D., Levizzani, V., Bortoli, D., Silva, A. M., and Pinto, P.: Modelling of orographic precipitation over Iberia: a springtime case study, Adv. Geosci., 25, 103–110, doi:10.5194/adgeo-25-103-2010, 2010.

Dettinger, M. D., Ralph, F. M., Das, T., Neiman, P. J., and Cayan, D. R.: Atmospheric Rivers, Floods and the Water Resources of California, Water, 3, 445–478, doi:10.3390/w3020445, 2011.

Gal-Chen, T. and Somerville, R. C. J.: On the use of a coordinate transformation for the solution of the Navier-Stokes equations, J. Comput. Phys., 17, 209–228, 1975.

Gregory, D., Morcrette, J.-J., Jakob, C., Beljaars, A. C. M., and Stockdale, T.: Revision of convection, radiation and cloud schemes in the ECMWF Integrated Forecasting System, Q. J. Roy. Meteor. Soc., 126, 1685–1710, 2000.

Houze Jr., R. A.: Cloud dynamics. Academic Press, 573 pp., 1993.

Kain, J. S. and Fritsch, J. M.: Convective parameterization for mesoscale models: The Kain-Fritsch scheme, Meteor. Monogr., 46, 165–170, 1993.

Kerns, B. W. J., Chen, Y. L., and Chang, M. Y.: The diurnal cycle of winds, rain, and clouds over Taiwan during the Mei-Yu, summer, and autumn rainfall regimes, Mon. Weather Rev., 138, 497–516, 2010.

Kirshbaum, D. J. and Smith, R. B.: Orographic precipitation in the tropics: Large-eddy simulations and theory, J. Atmos. Sci., 66, 2559–2578, doi:10.1175/2009JAS2990.1, 2009.

Kolivras, K. N. and Comrie, A. C.: Regionalization and variability of precipitation in Hawaii, Phys. Geogr., 28, 76–96, 2007.

Lafore, J. P., Stein, J., Asencio, N., Bougeault, P., Ducrocq, V., Duron, J., Fischer, C., Héreil, P., Mascart, P., Masson, V., Pinty, J. P., Redelsperger, J. L., Richard, E., and Vil'-Guerau de Arellano, J.: The Meso-NH Atmospheric Simulation System. Part I: adiabatic formulation and control simulations, Ann. Geophys., 16, 90–109, doi:10.1007/s00585-997-0090-6, 1998.

Lin, Y.-L., Chiao, S., Wang, T. A., Kaplan, M. L., and Weglarz, R. P.: Some common ingredients for heavy orographic rainfall, Weather Forecast., 16, 633–660, 2001.

Luna, T., Rocha, A., Carvalho, A. C., Ferreira, J. A., and Sousa, J.: Modelling the extreme precipitation event over Madeira Island on 20 February 2010, Nat. Hazards Earth Syst. Sci., 11, 2437–2452, doi:10.5194/nhess-11-2437-2011, 2011.

Masson, V., Champeaux, J. L., Chauvin, F., Meriguet, C., and Lacaze, R.: A global database of land surface parameters at 1 km resolution in meteorological and climate models, J. Climate, 16, 1261–1282, 2003.

Morcrette, J.-J.: Radiation and cloud radiative properties in the ECMWF operational weather forecast model, J. Geophys. Res., 96, 9121–9132, 1991.

Morcrette, J.-J., Smith, L., and Fouquart, Y.: Pressure and temperature dependence of the absorption in longwave radiation parametrizations, Beitr. Phys. Atmosph., 59, 455–469, 1986.

Neiman, P. J., Ralph, F. M., Wick, G. A., Lundquist, J., and Dettinger, M. D.: Meteorological characteristics and overland precipitation impacts of atmospheric rivers affecting the West Coast of North America based on eight years of SSM/I satellite observations, J. Hydrometeorol., 9, 22–47, 2008a.

Neiman, P. J., Ralph, F. M., Wick, G. A., Kuo, Y. H., Wee, T. K., Ma, Z., Taylor, G. H., and Dettinger, M. D.: Diagnosis of an intense atmospheric river impacting the Pacific Northwest-Storm summary and offshore vertical structure observed with COSMIC satellite retrievals, Mon. Weather Rev., 136, 4398–4420, 2008b.

Noilhan, J. and Planton, S.: A simple parameterization of land surface processes for meteorological models, Mon. Weather Rev., 117, 536–549, 1989.

Nuissier, O., Ducrocq, V., Ricard, D., Lebeaupin, C., and Anquetin, S.: A numerical study of three catastrophic precipitating events over Southern France, I: Numerical framework and synoptic ingredients, Q. J. Roy. Meteor. Soc., 134, 111–130, 2008.

Parkinson, C. L.: Aqua: An Earth-observing satellite mission to examine water and other climate variables, IEEE T. Geosci. Remote, 41, 173–183, 2003.

Pinty, J.-P. and Jabouille, P.: A mixed-phase cloud parameterization for use in a mesoscale non hydrostatic model: Simulations of a squall line and of orographic precipitation, in: Proceedings of Conference on Cloud Physics, 17–21 August 1998, Everett, USA, 217–220, 1998.

Prada, S. and Silva, M. O.: Fog precipitation on the island of Madeira (Portugal), Environ. Geol., 41, 384–389, 2001.

Prada, S., Sequeira, M. M., Figueira, C., and Silva, M. O.: Fog precipitation and rainfall interception in the natural forests of Madeira island (Portugal), Agr. Forest Meteorol., 149, 1179–1187, 2009.

Ralph, F. M., Neiman, P. J., and Wick, G. A.: Satellite and CALJET aircraft observations of atmospheric rivers over the eastern North-Pacific Ocean during the winter of 1997/98, Mon. Weather Rev., 132, 1721–1745, 2004.

Ralph, F. M., Neiman, P. J., Wick, G. A., Gutman, S., Dettinger, M., Cayan, D., and White, A. B.: Flooding on California's Russian River: The role of atmospheric rivers, Geophys. Res. Lett., 33, 5

pp., doi:10.1029/2006GL026689, 2006.

Richard, E., Chaboureau, J.-P., Flamant, C., Champollion, C., Hagen, M., Schmidt, K., Kiemle, C., Corsmeier, U., Barthlott, C., and Di Girolamo, P.: Forecasting summer convection over the Black Forest: A case study from the Convective and Orographically induced Precipitation Study (COPS) experiment, Q. J. Roy. Meteor. Soc., 137, 101–117, 2011.

Roe, G. H.: Orographic Precipitation, Annu. Rev. Earth Pl. Sc., 33, 645–671, 2005.

Rotunno, R. and Houze, R. A.: Lessons on orographic precipitation from the Mesoscale Alpine Programme, Q. J. Roy. Meteor. Soc., 133, 811–830, doi:10.1002/qj.67, 2007.

Salgado, R. and Le Moigne, P.: Coupling the FLake model to the Surfex externalized surface model, Boreal Environ. Res., 15, 231–244, 2010.

Santos, F. D. and Miranda, P.: Alterações climáticas em Portugal. Cenários, impactos e medidas de adaptação, Projecto SIAM II, Gradiva Publicações, Lisboa, 506 pp., 2006.

Smith, R. B.: The influence of mountains on the atmosphere, Adv. Geophys., 21, 87–230, 1979.

Smith, R. B.: Progress on the theory of orographic precipitation, Chapter 1 in: Special Paper 398: Tectonics, Climate, And Landscape Evolution, edited by: Willett, S. D., Hovius, N., Brandon, M., and Fisher, D., Geological Society of America, Boulder, Colorado, 1–16, 2006.

Smith, R. B. and Barstad, I.: A linear theory of orographic precipitation, J. Atmos. Sci., 61, 1377–1391, 2004.

Smith, R. B., Schafer, P., Kirshbaum, D. J., and Regina, E.: Orographic Precipitation in the Tropics: Experiments in Dominica, J. Atmos. Sci., 66, 1698–1716, 2009a.

Smith, R. B., Schafer, P., Kirshbaum, D., and Regina, E.: Orographic Enhancement of Precipitation inside Hurricane Dean, J. Hydrometeorol., 10, 820–831, 2009b.

Stein, J., Richard, E., Lafore, J. P., Pinty, J. P., Asencio, N., and Cosma, S.: High-resolution non-hydrostatic simulations of flash-flood episodes with grid-nesting and ice-phase parametrization, Meteorol. Atmos. Phys., 72, 203–221, 2000.

Stohl, A., Forster, C., and Sodemann, H.: Remote sources of water vapor forming precipitation on the Norwegian west coast at 60°N – A tale of hurricanes and an atmospheric river, J. Geophys. Res., 113, D05102, doi:10.1029/2007JD009006, 2008.

Tomé, R. and Miranda, P. M. A.: Simulações da precipitação orográfica na ilha da Madeira, 5° Simpósio de Meteorologia e Geofísica da APMG (Peniche, Portugal), 2007.

Wulfmeyer, V., Behrendt, A., Kottmeier, C., Corsmeier, U., Barthlott, C., Craig, G. C., Hagen, M., Althausen, D., Aoshima, F., Apagaus, M., Bauer, H.-S., Bennett, L., Blyth, A., Brandau, C., Champollion, C., Crewell, S., Dick, G., Di Girolamo. P., Dorninger, M., Dufournet, Y., Eigenmann, R., Engelmann, R., Flamant, C., Foken, T., Gorgas, T., Grzeschik. M., Handwerker, J., Hauck, C., Höller, H., Junkermann, W., Kalthoff, N., Kiemle, C., Klink, S., König, M., Krauss, L., Long, C. N., Madonna, F., Mobbs, S., Neininger, B., Pal, S., Peters, G., Pigeon, G., Richard, E., Rotach, M. W., Russchenberg, H., Schwitalla, T., Smith, V., Steinacker, R., Trentmann, J., Turner, D. D., van Baelen, J., Vogt, S., Volkert, H., Weckwerth, T., Wernli, H., Wieser, A., and Wirth, M.: The Convective and Orographically induced Precipitation Study (COPS): The scientific strategy, the field phase, and research highlights, Q. J. R. Meteorol. Soc, 137, 3–30, doi:10.1002/qj.752, 2011.

Yeh, H. C. and Chen, Y. L.: Characteristics of rainfall distributions over Taiwan during the Taiwan Area Mesoscale Experiment (TAMEX), J. Appl. Meteor., 37, 1457–1469, 1998.

Zhu, Y. and Newell, R. E.: A proposed algorithm for moisture fluxes from atmospheric rivers, Mon. Weather Rev., 126, 725–735, 1998.